2003

A continuous-time nonlinear dynamic predictive modeling method for Hammerstein processes

Derrick K. Rollins Sr.
Iowa State University, drollins@iastate.edu

Nidhi Bhandari
Iowa State University

Ashraf Maurice Bassily
Iowa State University

See next page for additional authors

A Continuous-Time Nonlinear Dynamic Predictive Modeling Method for Hammerstein Processes

Derrick K. Rollins,*,† Nidhi Bhandari,†,‡ Ashraf M. Bassily,§,∥ Gerald M. Colver,§,⊥ and Swee-Teng Chin#

Department of Chemical Engineering, 2114 Sweeney Hall, Department of Mechanical Engineering, 2036 Black Engineering, and Department of Statistics, 102 Snedecor Hall, Iowa State University, Ames, Iowa 50011

This paper extends the method introduced by Rollins et al. (*ISA Trans.* **1998**, *36*, 293) to multiple-input, multiple-output systems that give an exact closed-form solution to continuous-time Hammerstein processes written in terms of differential equations and nonlinear inputs. This ability is demonstrated on a theoretical nonlinear Hammerstein process of complex dynamics where perfect identification of the closed-form model is assumed. This paper then demonstrates the simplicity of the proposed identification procedure to obtain an accurate estimate of the exact model using a theoretical Hammerstein model. A powerful attribute of this methodology is the ability to make full use of the statistical design of experiments for optimal data collection and accurate parameter estimation. Application of the proposed method is demonstrated on a household clothes dryer with four input and five output variables. Only 27 trials (input changes) of a central composite design were needed for accurate model development of all five outputs over the input space, and the accurate predictive performance is demonstrated.

1. Introduction

Dynamic predictive models that address nonlinear behavior are essential for optimal operation and control of many processes. In recent years, dynamic models have been developed for a wide range of processes. Conventional approaches to explaining nonlinear behavior include modeling from theory or first principles,[2,3] using models linearized around steady state,[4−6] and developing data-driven or empirical models.[7,8] However, the approach that we propose here falls into none of these categories.

The proposed method has the ability to provide exact solutions to a class of block-oriented nonlinear dynamic systems called *Hammerstein processes* (see work by Billings[9]). The Hammerstein system combines linear dynamics with nonlinear steady-state gains. A description is shown in Figure 1 for a multiple-input, multiple-output (MIMO) system.

In terms of application, the dominant context (maybe exclusive context) of modeling Hammerstein processes has been discrete-time modeling which falls into the class of NARMAX (nonlinear autoregressive moving average with exogenous inputs) models. Pearson and Ogunnaike[10] point out that this popularity is related to the discrete environment of digital control, measurement, and sampling. However, this environment can cause some critical drawbacks for discrete-time modeling when sampling is infrequent, nonconstant, or not online.[11]

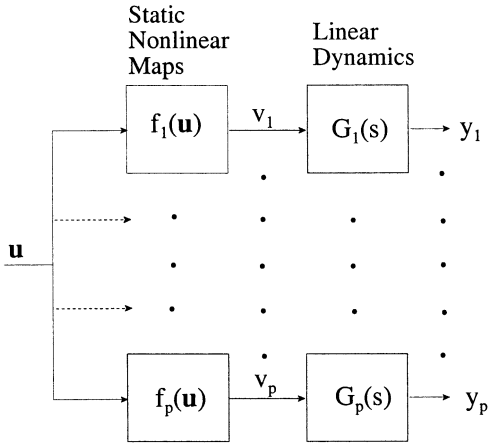

Figure 1. Description of the general "MIMO Hammerstein model" structure.[9] The input vector **u** passes through a static map and produces the gain vector **f**(**U**), which can be nonlinear, and then passes through the linear dynamic map **G**(*s*) and produces the output vector **y**.

The discrete-time identification results in "black-box" (i.e., empirical) identification for both the static nonlinear map and linear dynamics. Thus, depending on the sampling rate and the number of inputs, the number of parameters to be estimated can be quite large (can be more than several hundred and even in thousands[10]), making the model identification step quite a challenge. As pointed out by Eskinat et al.,[12] this situation is severely escalated when treating the more general case of all possible combinations and order of terms. In their work they did not consider the interaction of inputs (i.e., terms for product of input variables), which appears to be common practice.

* Corresponding author. E-mail: drollins@iastate.edu. Fax: 515-294-2689. Phone: 515-294-5516.
† Department of Chemical Engineering, 2114 Sweeney Hall.
‡ E-mail: nidhi@iastate.edu.
§ Department of Mechanical Engineering, 2036 Black Engineering.
∥ E-mail: bassily@iastate.edu. Fax: 515-294-3261.
⊥ E-mail: gmc@iastate.edu. Fax: 515-294-3261.
Department of Statistics, 102 Snedecor Hall. E-mail: sweete@iastate.edu. Fax: 515-294-2689.

10.1021/ie020169g CCC: $25.00
Published on Web 01/24/2003

The continuous-time method that we propose results in the identification of a "grey-box" (i.e., semiempirical model) for the dynamic block. Therefore, modeling and estimation is simpler because of the ease and simplicity of specifying these model forms, which have a small number of parameters (usually four at the most). Further, it does not suffer from limitations of discrete-time methods because it is a continuous-time method. Because the methodology is based on an exact solution to the block-oriented Hammerstein process, we call it the Hammerstein block-oriented exact solution technique or H-BEST.

The introduction of H-BEST (referred to as SET at that time) involved a single-input, single-output (SISO) study of a simulated continuous stirred tank reactor.[1] This study revealed its ability to predict excellently for a variety of output sampling situations including no sampling of the output. At that point its connection to a Hammerstein structure was not realized, and that discovery was made more recently. Rietz and Rollins[13] demonstrated the implementation of H-BEST into a real SISO continuous process connected to a distributed control system. Rollins et al.[14] displayed the ability of H-BEST to model complex dynamics (e.g., underdamped and inverse response) exceptionally well. H-BEST applications have not been limited to chemical processes. Walker[15] used it successfully in SISO modeling of a surrogate human's (i.e., a mathematical human model) thermoregulatory response to changes in ambient conditions.

The main objective of this paper is to demonstrate the effectiveness of H-BEST in modeling nonlinear MIMO systems that are Hammerstein or approximately Hammerstein in nature. In this work we determined how to effectively make this extension from a SISO system to a MIMO system. Critical questions that we have now answered include the model form to fully exploit information from statistical design of experiments (SDOE) and how to address interactions and other terms in model development. In addition, this is the first application of H-BEST to a batch process. This work also demonstrates the ability of H-BEST to model a real system.

This paper presents the proposed methodology in the following outline. The next section presents a closed-form exact solution to special cases of Hammerstein processes for step input changes (see the appendix for specific details). The methodology is developed from this solution and presented after the solution. Following this section, the proposed method is illustrated on theoretical Hammerstein processes. Finally, application is illustrated on a real process with four inputs and five outputs that involves the use of a central composite experimental design.

2. An Exact Solution

This section gives an exact solution for step input changes to Hammerstein systems as represented by Figure 1. This is the only compact closed-form continuous-time solution to our knowledge. The other types of solutions that we have found[16] have not been written in compact closed form. We illustrate our solution using the Hammerstein system given as

$$v(t) = f(\mathbf{U}(t),\boldsymbol{\beta}) = \beta_1 u_1(t) + \beta_2 u_2(t) + \beta_3 u_1(t)\, u_2(t) + \beta_4 u_1(t)^2 + \beta_5 u_2(t)^2 \quad (1)$$

$$\tau_1\tau_2 \frac{\mathrm{d}^2 y(t)}{\mathrm{d}t^2} + (\tau_1 + \tau_2)\frac{\mathrm{d}y(t)}{\mathrm{d}t} + y(t) = \tau_a \frac{\mathrm{d}v(t)}{\mathrm{d}t} + v(t) \quad (2)$$

where u and y are deviation variables. The exact solution we found to eqs 1 and 2 for a step change in the inputs at time 0 is given as

$$y(t) = f(\mathbf{U}(t{=}0);\boldsymbol{\beta})\, g(t;\boldsymbol{\tau}) \quad (3)$$

where

$$g(t;\boldsymbol{\tau}) = \mathscr{L}^{-1}\left(\frac{G(s)}{s}\right) = \mathscr{L}^{-1}\left(\frac{\tau_a s + 1}{\tau_1\tau_2 s^2 + (\tau_1 + \tau_2)s + 1}\frac{1}{s}\right) = \left[1 + \left(\frac{\tau_a - \tau_1}{\tau_1 - \tau_2}\right)\mathrm{e}^{-t/\tau_1} + \left(\frac{\tau_a - \tau_2}{\tau_2 - \tau_1}\right)\mathrm{e}^{-t/\tau_2}\right] \quad (4)$$

$$f(\mathbf{U}(t{=}0);\boldsymbol{\beta}) = \beta_1 u_1(0) + \beta_2 u_2(0) + \beta_3 u_1(0)\, u_2(0) + \beta_4 u_1(0)^2 + \beta_5 u_2(0)^2 \quad (5)$$

$G(s) = Y(s)/V(s)$, and $\mathscr{L}^{-1}$ is the inverse Laplace transform operator. Combining eqs 4 and 5 gives

$$y(t) = [\beta_1 u_1(0) + \beta_2 u_2(0) + \beta_3 u_1(0)\, u_2(0) + \beta_4 u_1(0)^2 + \beta_5 u_2(0)^2]\cdot\left[1 + \left(\frac{\tau_a - \tau_1}{\tau_1 - \tau_2}\right)\mathrm{e}^{-t/\tau_1} + \left(\frac{\tau_a - \tau_2}{\tau_2 - \tau_1}\right)\mathrm{e}^{-t/\tau_2}\right] \quad (6)$$

A mathematical proof of the exactness of the solution is given in the appendix. To test our claim that eq 6 exactly solves eqs 1 and 2, one can specify their own functions [$f(u)$ and $G(s)$] and the value for $u(0)$, solve eqs 1 and 2 numerically over some time period, and compare the results using eq 6. In our experiments, we have found the results to give exact agreement. We give an example of this agreement following the next discussion.

Although the solution of a Hammerstein process for a single-input change is an advancement, a more practical outcome is a solution to a series of changes in input over time, as given by eq 7.

$$\begin{aligned} &0 \le t < t_1, \quad u(t) = u(0) \\ &t_1 \le t < t_2, \quad u(t) = u(t_1) \\ &t_2 \le t < t_3, \quad u(t) = u(t_2) \\ &\vdots \qquad\qquad \vdots \end{aligned} \quad (7)$$

We provide this solution in the form of the algorithm we have developed in eq 8.

$$\begin{aligned} &0 \le t < t_1, \quad y(t) = f(U(t{=}0);\boldsymbol{\beta})\, g(t;\boldsymbol{\tau}) \\ &t_1 \le t < t_2, \\ &\qquad y(t) = y(t_1) + [f(\mathbf{U}(t{=}t_1);\boldsymbol{\beta}) - y(t_1)]\, g(t{-}t_1;\boldsymbol{\tau}) \\ &t_2 \le t < t_3, \\ &\qquad y(t) = y(t_2) + [f(\mathbf{U}(t{=}t_2);\boldsymbol{\beta}) - y(t_1)]\, g(t{-}t_2;\boldsymbol{\tau}) \\ &\vdots \qquad\qquad\qquad\qquad \vdots \end{aligned} \quad (8)$$

We have found this algorithm to give an exact solution for Hammerstein processes without the restriction of steady state between input changes for nth-order overdamped dynamic systems. For details of this proof, see

the appendix. In all other cases, the accuracy will depend on the level of complexity of dynamic behavior and the rate of input changes, as described in the appendix.

The solution presented above has several advantageous attributes. The solution identifies the functions (f and g) and retains them in their original form. The solution is compact and easily useable. Other continuous-time solutions are usually expressed as integral equations, which can be quite challenging to solve to get closed-form solutions. Defining attributes of the H-BEST solution are its ease and simplicity in arriving at its solution.

3. Proposed Methodology (H-BEST)

In this section we present a methodology to obtain estimates of the linear and dynamic model forms and their parameters in eq 6 when modeling real systems from data. In the last section we saw that the form of the static nonlinear function [i.e., the $f(\cdot)$] is preserved in the exact solution we presented. This result is exploited by H-BEST for model building in several ways. First, the modeling of this function is allowed to be separate from the modeling of the dynamic function [i.e., the $g(\cdot)$]. Second, because the determination of $f(\cdot)$ is separate, model specification and optimal data collection can be driven in a conventional statistical manner. More specifically, because this is steady-state modeling and fitting, one is able to take full advantage of the field of SDOE. Third, if $f(\cdot)$ can be mathematically represented, then it can be modeled, along with any steady-state function, using statistical methods. Thus, there are no restrictions on the form of $f(\cdot)$.

In the last section we also saw that the forms of the dynamic terms were written in the time domain and represented conventional dynamic processes with a step input change (see eq 4). This result is also exploited by H-BEST for model building as follows. The input changes that are determined by SDOE for obtaining $f(\cdot)$ are used as step changes, and the dynamic data are used to determine $g(\cdot)$. Because these model forms are nonlinear in the parameters, nonlinear regression is used to estimate their values.

The specific steps for model building are as follows:

1. Determine the statistical experimental design.

2. Run the experimental design as a series of step tests, allowing steady state to occur after each change and collecting the data dynamically over time.

3. Use the steady-state data to determine the ultimate response function, $f(\Delta\mathbf{u};\boldsymbol{\beta})$, for each output. $\Delta\mathbf{u}$ is a deviation variable, i.e., $\Delta\mathbf{u}(t) = \mathbf{u}(t) - \mathbf{u}_{ss}$.

4. Use the dynamic data to determine the dynamic response function, $g(t;\boldsymbol{\tau})$, for each output.

In the first step, the selected SDOE is based on steady-state modeling and, thus, is the same one that one would select based strictly on fitting *only* $f(\Delta\mathbf{u};\boldsymbol{\beta})$. That is, H-BEST does not require any additional SDOE knowledge over that contained in standard statistical textbooks on SDOE.[17] The design that one selects is dependent on the a priori assumptions regarding the nonlinear and interactive ultimate response behavior, as well as cost considerations. The second step is data collection. For each experimental trial or step test, the input changes are made, and dynamic data for each output are collected over time from the time of the change until the process settles.

In the third step the input changes are collected with the ultimate response values for each output, and a fitted $f(\Delta\mathbf{u};\boldsymbol{\beta})$ is obtained for each output. These functions are then set aside while the dynamic data, in step 4, are used to estimate $g(t;\boldsymbol{\tau})$ for each output. As stated above, because these forms are usually nonlinear in the τ's, nonlinear regression techniques are needed to determine their estimates.

Note that, for a given output, there will be one fit for each trial. Thus, there is the possibility of finding different order functions for different trials for the same output. In these cases, we recommend selecting the highest order form for a given output and fitting each trial to this form. After completely obtaining the fitted $g(t;\boldsymbol{\tau})$ for each output, one can fit $\boldsymbol{\tau}$ over the input space for each response using multiple linear regression. However, we have found $\boldsymbol{\tau}$ to be fairly robust in many cases, making this requirement unnecessary. Hence, in most cases the average values from all of the trials for $\boldsymbol{\tau}$ is sufficient. Note that the Hammerstein structure (see Figure 1) has one dynamic form associated with one output. By using a model to vary $\boldsymbol{\tau}$ as the inputs vary, this is essentially allowing the dynamic structure to change with the input level which, strictly speaking, is outside the scope of the Hammerstein structure. In the situation when even this is not adequate to address changing dynamics with input changes, one will certainly have to consider a structure beyond Hammerstein, which is outside the scope of this methodology. We have addressed these situations in research by using Wiener and more complex block-oriented structures with promising results.

The above procedure to fit $f(\Delta\mathbf{u};\boldsymbol{\beta})$ and $g(t;\boldsymbol{\tau})$, separately, has also been applied in discrete-time Hammerstein modeling.[12] In addition, one must understand that the emphasis of H-BEST is not system identification. System identification is the fitting of $f(\Delta\mathbf{u};\boldsymbol{\beta})$ and $g(t;\boldsymbol{\tau})$, which is typically not a difficult task for our approach. For real systems, the approximate fitting of $f(\Delta\mathbf{u};\boldsymbol{\beta})$ can often be done fairly accurately using the method of linear regression. The identification of $g(t;\boldsymbol{\tau})$ can typically be done by inspection and a knowledge of how first- and second-order systems behave, which is found in any first course textbook in process control. If the function is not well behaved, system identification might become more of a challenge, but this is beyond the scope of this paper.

After the fitted equations for $f(\Delta\mathbf{u};\boldsymbol{\beta})$ and $g(t;\boldsymbol{\tau})$ are obtained, they are incorporated into the algorithm (i.e., eq 8) to predict the output response for changes in inputs. We discovered the proposed algorithm after several failed attempts (see Bhandari and Rollins[18] for an earlier version). Although simple in form, the prediction algorithm is an extremely critical component of the methodology. Without it, even with accurate fits for $f(\Delta\mathbf{u};\boldsymbol{\beta})$ and $g(t;\boldsymbol{\tau})$, prediction would not be accurate. It is now given in a more general framework and described in more detail than before.

The H-BEST algorithm is a procedure that predicts the output response from the fits for $f(\Delta\mathbf{u};\boldsymbol{\beta})$ and $g(t;\boldsymbol{\tau})$ in a scheme that depends only on the most recent change for each input. The advantage of using the most recent input change for each variable is greater accuracy when modeling errors and measurement errors can propagate over time.[18] For an input step change occurring at time t_1, a more general representation of the H-BEST prediction algorithm is given by eq 9 as

For $t > t_1$: $\hat{y}(t) = \hat{y}(t_1) + [f(\Delta\mathbf{u}(t_1);\hat{\boldsymbol{\beta}}) - \hat{y}(t_1) + y(0)]g((t-t_1);\hat{\boldsymbol{\tau}})\ \mathbf{S}(t-t_1)$ (9)

where $\hat{y}(t)$ is the predicted output response at time t; $y(0)$ is the measured value of the output at the initial time, 0; $\Delta\mathbf{u}(t_1)$ is a vector that contains the deviation values of the process variables from their steady-state values at time $t = 0$, i.e., $\Delta\mathbf{u}(t_1) = \mathbf{u}(t) - \mathbf{u}_{ss}$; $\hat{\boldsymbol{\beta}}$ is a vector that contains the estimates of the steady-state response parameters determined from the current input conditions; $f(\Delta\mathbf{u}(t_1);\hat{\boldsymbol{\beta}})$ is the function that computes the change in the ultimate response for the change $\Delta\mathbf{u}(t_1)$; $\hat{\boldsymbol{\tau}}$ is a vector that contains the estimates of the dynamic parameters that could depend on $\Delta\mathbf{u}(t_1)$; $g(t-t_1;\hat{\boldsymbol{\tau}})$ is the semiempirical nonlinear function that computes the dynamic portion of the response such that as $t \rightarrow \infty$, the function $\rightarrow 1$; and $\mathbf{S}(t-t_1)$ is the shifted unit step function. Note that, at t_1, $\hat{y}(t) = \hat{y}(t_1)$, and as $t \rightarrow \infty$, $\hat{y}(t) \rightarrow y(0) + f(\Delta\mathbf{u}(t_1);\hat{\boldsymbol{\beta}})$. Thus, the algorithm provides proper initial and limiting behavior. See Rietz and Rollins[13] for a modification of the algorithm to include online measured output data. However, because measurement noise is filtered (because of the smoothing nature of the predictive function) during parameter estimation, only in situations of very high measurement inaccuracy will the use of output data give modest improvement in accuracy over the unmeasured situation.[19] Next, we illustrate the application of this methodology on a theoretical process.

4. Application of H-BEST to the Theoretical Hammerstein Process

In this section we present the application of H-BEST to a theoretical Hammerstein process presented by Haber and Unbehauen,[20] to clearly delineate the steps involved. Their Hammerstein system, which has one input and one output, is given by eq 10 as

$$v(t) = 2.0 + u(t) + 0.5u(t)^2$$

$$10\frac{dy(t)}{dt} + y(t) = v(t) \qquad (10)$$

with $u_{ss} = 0$ and $y_{ss} = 2.0$. In this section, we will also demonstrate the ability of H-BEST to estimate the parameters in eq 10 and the correct forms for eq 10. Note that for this case the correct forms are

$$f(\Delta u;\beta) = f(u;\beta) = u(t) + 0.5u(t)^2 \qquad (11)$$

$$g(t;\tau) = 1 - e^{-t/10} \qquad (12)$$

One measure of the soundness of this approach will be its ability to accurately obtain eqs 11 and 12. The other critical measure will be to obtain accurate predictions over time for changes in $u(t)$ through the use of eq 9.

The first step in applying H-BEST is to determine the experimental design. Because this is a SISO process and the ultimate response is quadratic, the following four input changes were chosen as the experimental design: $u = -4$, -1, 1, and 4. These input changes were made, and the fits shown in Figure 2 were obtained using first-order models.

As shown, the fit to each step test is quite accurate. From each trial (i.e., the change in u), the ultimate response value was obtained and used to estimate eq 11. Figure 3 shows a plot of the ultimate response data versus u. Five points are shown which include the four design points and the center point ($u = 0$). This figure demonstrates the highly nonlinear behavior of the ultimate response over this input space. Fitting a quadratic model to data in Figure 3 using linear regression produced the following, excellent, approximation of eq 11.

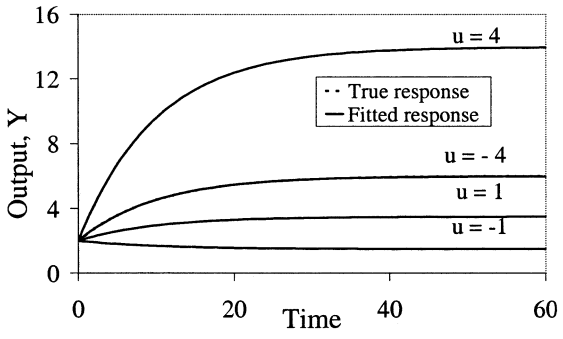

Figure 2. Response of Y and the fits of the first-order models for the four changes in u to obtain estimates of eqs 11 and 12.

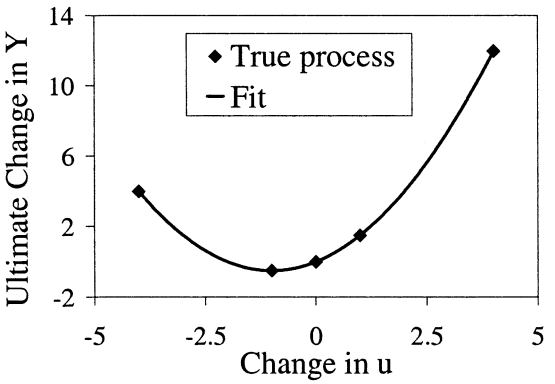

Figure 3. Plot of the ultimate change in Y against u with the fitted line (eq 13) for the changes in the u.

$$f(u;\hat{\beta}) = 0.998u(t) + 0.499u(t)^2 \qquad (13)$$

The four estimates of τ from each of the first-order fits in Figure 2 were averaged to obtain the estimate for eq 12. This value was 9.93, giving a close estimate of eq 12 as shown.

$$g(t;\hat{\tau}) = 1 - e^{-t/9.93} \qquad (14)$$

Testing H-BEST for this process consisted of incorporating the estimates of eqs 11 and 12 into eq 9 and examining its predictive behavior when making arbitrary changes in u over the fitted input space. The input change sequence for this test is shown in Figure 4. The process response and the response of H-BEST for this input sequence change are presented in Figure 5. As shown, H-BEST predicts almost perfectly the real process. This follows from the fact that H-BEST gives an exact solution to the true Hammerstein process and this methodology was able to estimate the parameters accurately. That is, if the true functions (eqs 11 and 12) were incorporated into eq 9, its agreement with the true process would have been perfect.

Similarly, to obtain accurate predictions for the process described by eqs 1 and 2, one could choose an appropriate design that allows for estimation of quadratic effects for two inputs such as a three-level

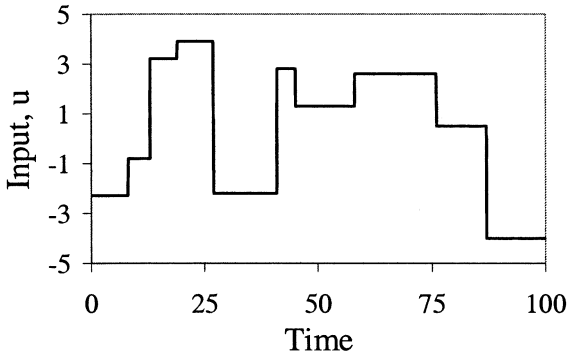

Figure 4. Input sequence for testing H-BEST for the first-order Hammerstein process.

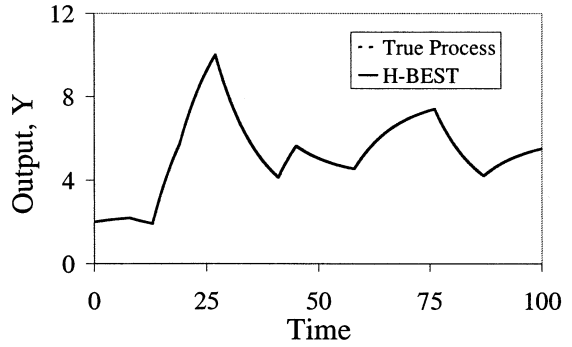

Figure 5. Predictions from H-BEST for the input testing sequence of Figure 4.

factorial design. Then one would use the steady state and the dynamic data from these step tests to obtain estimates of β and τ and last use eq 9 to obtain accurate predictions. In the following sections, we present the details of the dryer and the procedure followed to obtain predictive models for the dryer responses using H-BEST.

5. Experimental Setup for the Dryer

Figure 6 shows a schematic of the dryer and its instrumentation. The process is a common household-style dryer that has been retrofitted with additional sensors and measuring and recording instruments. The air flow rate is measured at the inlet of the electric heater using a standard flow nozzle with a known flow coefficient and a standard nozzle box to ensure uniform streamlines at the nozzle inlet. An additional fan is installed at the box inlet to overcome the pressure losses across the nozzle box and the flow nozzle and used to change the inlet mass flow rate during the investigation of the effect of the inlet mass flow rate on the mass-transfer coefficient. The air flow rate is also measured at the dryer outlet for the investigation of the mass-transfer coefficient using a flow nozzle.

The coil surface temperatures are measured at six locations across the coil using K-type thermocouples that are welded on the coil surfaces. The instantaneous power supplied to the heater is determined by multiplying the measured voltage across the heater terminals and the current through the heater. The voltage across the heater terminals is measured using a voltage divider circuit to reduce the measured voltage to a maximum value of 5 V, which does not damage the data acquisition system. The current through the heater is measured using a 100 MV/15 A General Electric calibrated high resistor. A Duncan MR-2SU kilowatt-hour meter is used to measure the energy usage of the dryer and also to validate the instantaneous power reading.

Air temperatures are measured at many locations along the air path. Two K-type thermocouples are used to measure the inlet air temperature. Eight shielded K-type thermocouples are used to measure the air temperatures across the coils. Five K-type thermocouples at one section are used to measure the air temperatures at the heater outlet.

Using the average value of the air temperature at the heater outlet, the air temperature at the heater inlet, and the measured inlet flow rate, the output energy of the heater and the heater efficiency can be determined. Many K-type thermocouples are welded on the heater surface to approximately evaluate the energy losses from the heater so that the heater efficiency can be determined to validate the heater efficiency determined using the air flow rate and temperatures.

The relative humidity is measured at two locations inside the drum and at the dryer outlet. The relative humidity is determined by measuring the dry bulb temperature and the wet bulb temperature using K-type thermocouples and determining the corresponding relative humidity. The moisture content of the clothes is determined by weighing the bone-dry clothes and the wet clothes using a digital scale. A data acquisition system with a SCXI-1000 chassis with two modules is used to sample the measured data. The output of the thermocouples that are welded on the coil surfaces, the output voltage of the circuit divider, and the output voltage of the current resistor are connected to a high-voltage, eight-channel isolated analogue input SCXI-1120 module. The output voltages of the rest of the thermocouples are connected to a 32-channel thermocouple amplifier SCXI-1102 module. A Lab View program[21] written for an E3100-Gateway2000 computer was used to regulate the sampling and record the sampled data.

6. Experimental Design and Model Development

This section describes the sequential procedure that we used to obtain the fitted semiempirical models for the dryer process. The first step was the selection of the input variables. This selection involved identifying all of the variables that affected the process that could be manipulated and controlled. Ambient temperature and humidity affected the drying process but were not controlled. The input variables we chose for this study were the power supplied to the heater (P), the inlet fan speed (N), the dry weight of the clothes in the dryer (w), and the initial moisture content of the clothes (m). The output variables we chose for this study were the coil temperature (T_c), the air temperature of the air exiting the heater (T_a), the temperature of the heater surface (T_s), the dry bulb temperature of the air exiting the dryer (T_d), and the wet bulb temperature of the air exiting the dryer (T_w). The first three output variables are of interest, for example, during the optimum operation of the dryer because these would provide the constraints or bounds for the safe operation of the dryer. The last two output variables would be used to determine the relative humidity at the dryer exit and hence provide information about the extent of drying.

The next step required specifying the input space, sometimes also referred to as the operability region. The lower and upper limits on the input variable were chosen so that they covered a broad range. Within the

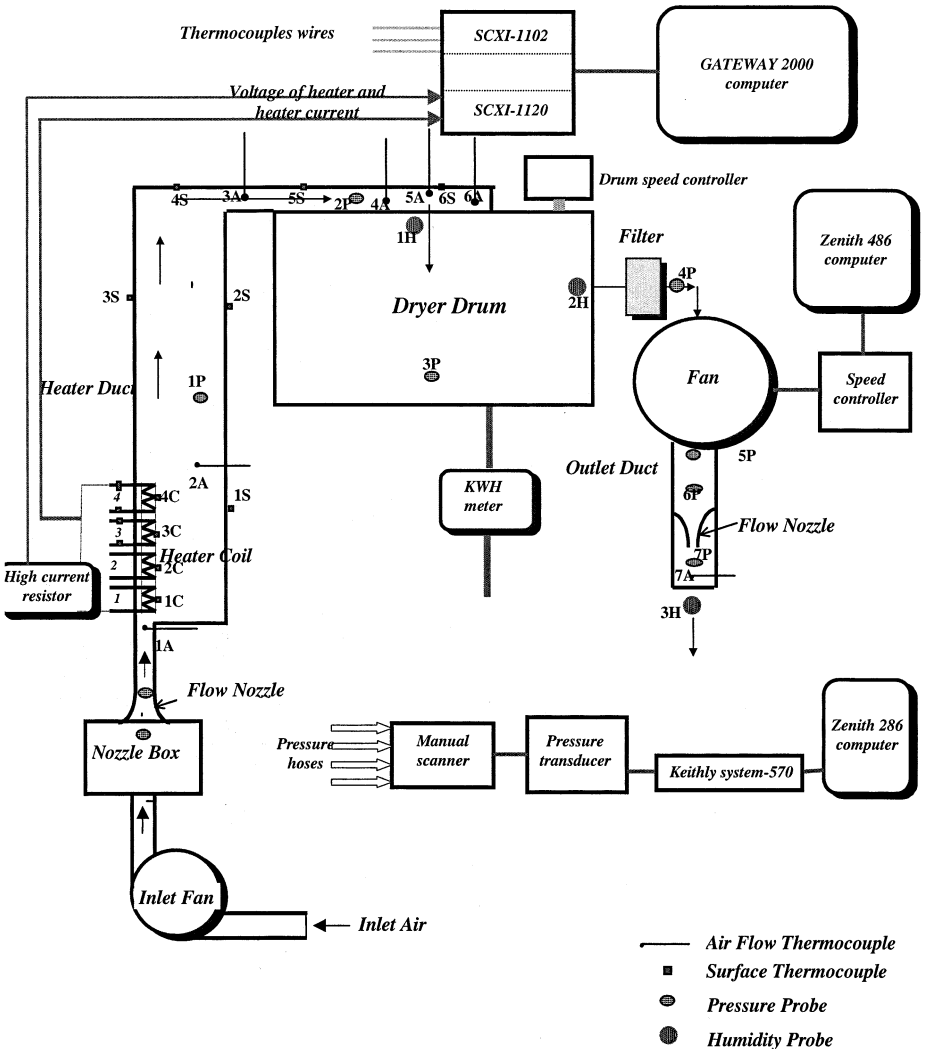

Figure 6. Schematic diagram of the dryer and its instrumentation.

Table 1. Five Levels for Each Input Variable

	coded level				
input (units)	−2	−1	0	1	2
power (W)	2000	2500	3000	3500	4000
fan speed (rpm)	1000	1250	1500	1750	2000
weight (kg)	1.82	2.27	2.72	3.18	3.63
moisture (%)	55	60	65	70	75

range of a variable, different levels were considered to model curvilinear effects across the input space. A complete factorial design, which allows detection and modeling of all possible interactions, to study the effects of four inputs (or factors) at five levels requires $5^4 = 625$ trials, which, obviously, is unrealistic for this process. Hence, we chose an optimal design that enables the testing and estimation of all two-factor interactions and quadratic effects. The experimental design meeting the criteria of our study for the dryer process was a central composite design with replicated center points.[17] Our design consisted of five levels for each input variable which we designated from low to high (i.e., coded) as −2, −1, 0, 1, and 2. The values for each level are given in Table 1.

The total number of experimental trials (i.e., runs) for our design was 27. This design consisted of 16 corner points, 8 star points, and 3 center points. The corner points are the 2^4 factorial design points considering the effect of four inputs at two levels (−1 and 1) each. The star points look at the effect of each input, at extreme levels (−2 and 2) while keeping the rest of the inputs at their middle levels. The center point implies setting each input to level 0 and was replicated in this study to give an estimate of the standard error. The 27 design points are given in Table 2. As stated above, this central composite design enables us to account for the two-factor interactive and nonlinear effects of the inputs on the output responses.

Each experiment consisted of starting the dryer with the input variables set to values for that run and then recording the outputs dynamically. Because of the batch nature of the dryer, the process does not reach steady state, but the output variables tend to level off. The drying process can be divided into two distinct phenomena: the constant-rate drying and the falling-rate drying. For our study, we considered only the constant-rate drying period. The transfer functions or the dynamic model forms were selected by a visual inspection of the dynamic response of the outputs. In cases where more than one transfer function could be used to adequately describe the process, the dynamic model with the smallest sum of square of error (SSE) was selected. We found that the dynamic response of any output was the same for all of the trials or runs but the estimates of dynamic parameters varied from one trial to the next trial. The dynamic parameters for the individual trials in the design are presented in work by

Table 2. Experimental Design Runs Conducted in This Study

run no.	power (W)	fan speed (rpm)	weight (kg)	moisture (%)
1	3506	1250	3.19	70.1
2	2937	1500	2.70	65.2
3	2534	1250	3.19	70.3
4	3641	1250	2.24	60.5
5	3559	1750	3.19	60.0
6	2970	1000	2.70	65.0
7	2987	1500	3.65	65.4
8	3650	1750	2.24	60.8
9	2556	1750	3.17	59.8
10	3633	1250	2.24	70.6
11	2638	1250	2.27	60.0
12	2563	1250	3.17	60.0
13	2954	2000	2.70	65.0
14	2535	1750	2.24	70.4
15	2925	1500	2.70	65.4
16	3643	1750	2.24	70.1
17	2968	1500	2.70	76.0
18	3001	1500	2.70	53.3
19	3977	1500	2.70	64.6
20	3568	1750	3.19	69.1
21	2955	1500	1.81	65.7
22	2457	1750	2.24	59.5
23	1995	1500	2.70	65.6
24	2940	1500	2.70	66.3
25	3555	1250	3.19	59.2
26	2488	1250	2.24	69.1
27	2532	1750	3.19	69.7

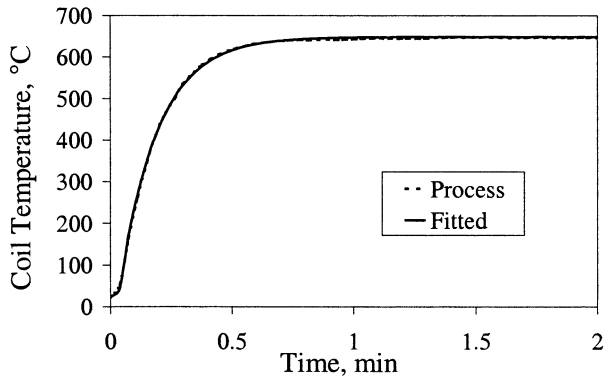

Figure 7. Dynamic response of the coil temperature for run 10. The fitted curve is generated by using an FO model and the parameter (τ_c) is estimated using nonlinear regression.

Bhandari.[22] The dynamic parameters for each output did not vary significantly over the input space, and the mean value of the parameter was used over the entire space. The linear dynamic model forms we chose for the five output variables were as follows: (i) coil temperature, first-order (FO) model; (ii) air temperature at the heater exit, second-order plus lead (SOPL) model; (iii) heater surface, first-order plus dead time (FOPDT) model; (iv) wet bulb temperature at the dryer outlet, SOPL plus dead time (SOPLPDT) model; (v) dry bulb temperature at the dryer outlet, FOPDT model.

The dynamic responses of the output variables (for one particular run, run 10) are shown in Figures 7−11. The fitted responses for other runs show the same excellent behavior but with different parameter estimates obtained for each run. The coil temperature response is shown in Figure 7, the air temperature at heater exit is shown in Figure 8, and the heater surface response is shown in Figure 9. The wet bulb temperature and the dry bulb temperature at the dryer outlet are shown in Figures 10 and 11, respectively. In all, for this five-output study with 27 trials, we fit 135 dynamic models (i.e., 5 outputs times 27 runs). Figures 7−11 also give the typical performances for these fits.

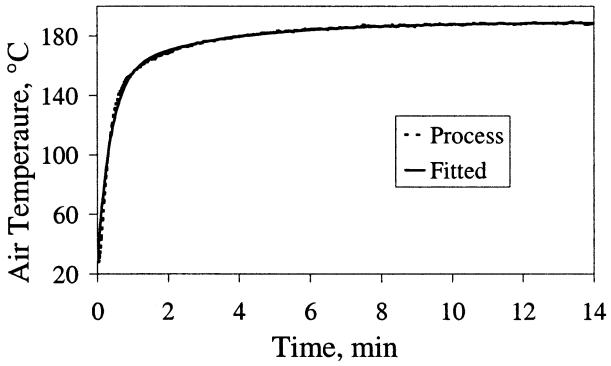

Figure 8. Dynamic response of the air temperature at the heater exit for run 10. The fitted curve is obtained by using a SOPL model, and the parameters (τ_{aa}, τ_{a1}, and τ_{a2}) are estimated by nonlinear regression.

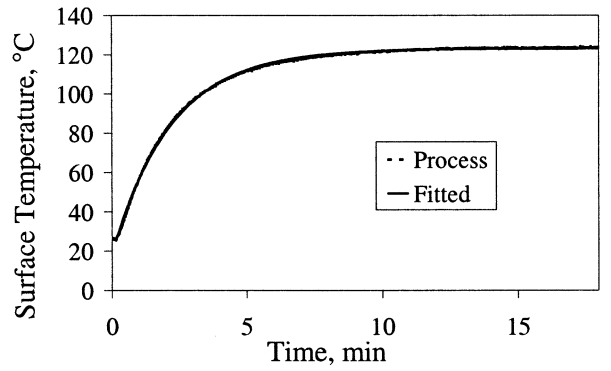

Figure 9. Dynamic response of the heater surface temperature for run 10. The fitted curve is generated by choosing an FOPDT model, and the parameters (τ_s and θ_s) are estimated by nonlinear regression.

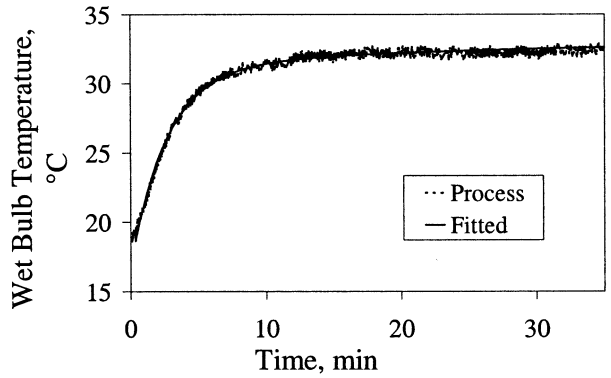

Figure 10. Response of the wet bulb temperature at the dryer outlet for run 10. The fitted curve is generated by choosing a SOPLPDT model. The parameters (τ_{wa}, τ_{w1}, τ_{w2}, and θ_w) are estimated by nonlinear regression.

The dynamic parameters (the τ's and θ's) for the dynamic models are obtained using nonlinear regression on the dynamic responses for each run. The dynamic parameters might change with the change in process conditions, and linear regression can be used to account for that dependence. In this case, the dynamic parameters did not vary much over the input space and thus the mean value from the runs was used. The average values of the dynamic parameters used in the H-BEST models are given in Table 3.

The ultimate changes, in the output variables for all of the runs, were modeled using linear regression techniques as a function of the input variables. The ultimate changes can be modeled using linear regression

with main effects, quadratic effects, and two-factor interactions. For each output, we started with the full model with linear, quadratic, and two-factor interaction terms and reduced the number of terms to retain only those statistically significant at the 0.05 level. The multiple coefficient of determination, R^2, values for the models were in the range of 80−85%.

Mathematically, the H-BEST models for the output responses are given below. Note that any output response is of the general form given by eq 15 as

$$T_i(t) = T_{i,0} + f_i(P,N,w,m)\, g_i(t;\hat{\boldsymbol{\tau}}) \tag{15}$$

where the first term, $T_{i,0}$, is the initial value of the output variable. The term $f_i(P,N,w,m)$ denotes the ultimate change in the ith output; i.e., it is the change in the output variable from its initial value to its new steady-state value as it time goes to ∞ and is given by the static gain or the ultimate change function. The last term, $g_i(t;\hat{\boldsymbol{\tau}})$, gives the time dependency of that change for each of the outputs and is given by the dynamic model.

The ultimate change and the dynamic functions for the five output responses are given in eqs 16−25:

Coil temperature:

$$f_c(P,N,w,m) = 3.73 \times 10^3 - 2.20 \times 10^{-1}P - 4.56 \times 10^{-1}N - 6.96 \times 10^2 w - 5.69 \times 10^1 m + 5.84 \times 10^{-5}P^2 + 1.49 \times 10^{-4}N^2 + 1.31 \times 10^2 w^2 + 4.32 \times 10^{-1}m^2 \tag{16}$$

$$g_c(t;\hat{\boldsymbol{\tau}}) = 1 - e^{-1/\hat{\tau}_c} \tag{17}$$

Air temperature:

$$f_a(P,N,w,m) = 1.22 \times 10^3 - 1.10 \times 10^{-1}P - 4.57 \times 10^{-3}N - 3.10 \times 10^2 w - 1.76 \times 10^1 m + 2.48 \times 10^{-5}P^2 + 5.76 \times 10^1 w^2 + 1.32 \times 10^{-1}m^2 \tag{18}$$

$$g_a(t;\hat{\boldsymbol{\tau}}) = 1 + \left(\frac{\hat{\tau}_{aa} - \hat{\tau}_{a1}}{\hat{\tau}_{a1} - \hat{\tau}_{a2}}\right)e^{-t/\hat{\tau}_{a1}} + \left(\frac{\hat{\tau}_{aa} - \hat{\tau}_{a2}}{\hat{\tau}_{a2} - \hat{\tau}_{a1}}\right)e^{-t/\hat{\tau}_{a2}} \tag{19}$$

Surface temperature:

$$f_s(P,N,w,m) = 3.79 \times 10^2 - 4.90 \times 10^{-2}P - 3.74 \times 10^{-3}N - 2.02 \times 10^2 w - 3.31 \times 10^{-1}m + 1.37 \times 10^{-5}P^2 + 3.72 \times 10^1 w^2 \tag{20}$$

$$g_s(t;\hat{\boldsymbol{\tau}}) = 1 - e^{-(t-\hat{\theta}_s)/\hat{\tau}_s} \tag{21}$$

Wet bulb temperature:

$$f_w(P,N,w,m) = 5.05 \times 10^0 - 5.88 \times 10^{-3}P - 2.73 \times 10^{-2}N - 3.62 \times 10^1 w - 5.34 \times 10^{-2}m - 8.72 \times 10^{-6}N^2 + 7.09 \times 10^{-6}PN + 7.14 \times 10^{-4}Nw - 6.55 \times 10^{-3}Nw - 4.42 \times 10^{-1}wm \tag{22}$$

$$g_w(t;\hat{\boldsymbol{\tau}}) = 1 + \left(\frac{\hat{\tau}_{wa} - \hat{\tau}_{w1}}{\hat{\tau}_{w1} - \hat{\tau}_{w2}}\right)e^{-(t-\hat{\theta}_w)/\hat{\tau}_{w1}} + \left(\frac{\hat{\tau}_{wa} - \hat{\tau}_{w1}}{\hat{\tau}_{w2} - \hat{\tau}_{w1}}\right)e^{-(t-\hat{\theta}_w)/\hat{\tau}_{w2}} \tag{23}$$

Dry bulb temperature:

$$f_d(P,N,w,m) = 5.71 \times 10^1 - 5.31 \times 10^{-3}P + 1.49 \times 10^{-2}N + 1.11 \times 10^1 w - 1.92 \times 10^0 m + 1.75 \times 10^{-6}P^2 + 3.51 \times 10^0 w^2 + 2.18 \times 10^{-2}m^2 - 6.88 \times 10^{-3}Nw - 3.42 \times 10^{-1}wm \tag{24}$$

$$g_d(t;\hat{\boldsymbol{\tau}}) = 1 - e^{-(t-\hat{\theta}_d)/\hat{\tau}_d} \tag{25}$$

where the outputs, T, are in °C, power, P, is in W, fan speed, N, is in rpm, weight of clothes, w, is in kg, and moisture content, m, is in wt %. As mentioned previously, the estimates for the dynamic parameters are presented in Table 3. In the next section, we present the incorporation of the nonlinear gain and dynamic models into the H-BEST algorithm to generate output predictions for a series of input changes.

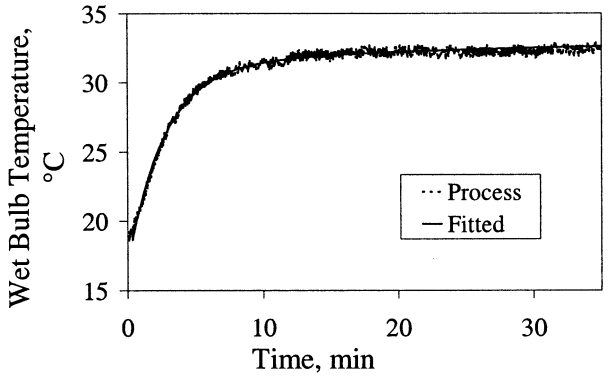

Figure 11. Dynamic response of the dry bulb temperature at the dryer outlet for run 10. The fitted curve is generated by choosing an FOPDT model, and the parameters (τ_d and θ_d) are estimated by nonlinear regression.

Table 3. Estimates of the Dynamic Parameters

parameter (units)	estimate (min)	parameter (units)	estimate (min)	parameter (units)	estimate (min)
τ_c	0.163	τ_s	2.214	τ_{w2}	4.877
τ_{aa}	3.035	θ_s	0.155	θ_w	0.465
τ_{a1}	0.389	τ_{wa}	59.684	τ_d	3.653
τ_{a2}	3.623	τ_{w1}	53.018	θ_d	0.736

7. H-BEST Algorithm

The use of semiempirical model forms in the H-BEST algorithm is a major step of this approach. The algorithm creatively modifies the dynamic prediction equation (eq 15) each time an input change occurs. For the sake of illustration, let us consider that the starting values of the power, fan speed, weight of clothes, and moisture content are P_0, N_0, w_0, and m_0, respectively. Further, the power value then changes to P_1, the change occurs at time t_{P_1}, and the first change in fan speed occurs later at time t_{N_1}, changing its value to N_1. Similarly, the second change in power occurs at time t_{P_2}, and the second change in fan speed occurs later than t_{P_2} at time t_{N_2} so that the power and the fan speed values are P_2 and N_2, respectively. Let Y be any output variable, ΔY^∞ be the ultimate change function, and

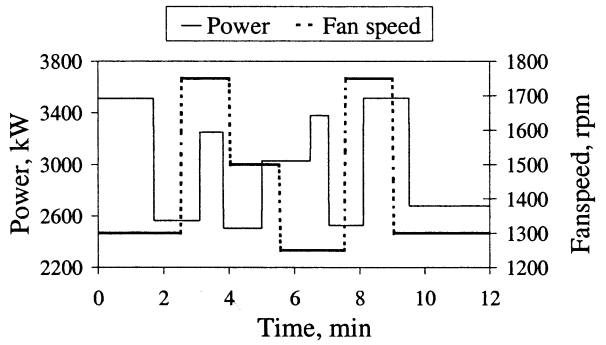

Figure 12. Input sequences, for power and fan speed, used for the study.

$g(t,\hat{\boldsymbol{\tau}}_y)$ be its corresponding semiempirical fitted model. Mathematically, for this scenario, the algorithm is represented as follows:

For $t \le \hat{\theta}_y$

$$\hat{Y} = Y_0$$

For $\hat{\theta}_y < t \le t_{P_1} + \hat{\theta}_y$

$$\hat{Y} = Y_0 + [\Delta Y^{\infty}(P_0,N_0,w_0,m_0;\hat{\beta}_y)]g((t-\hat{\theta}_y),\hat{\tau}_y)$$

For $t_{P_1} + \hat{\theta}_y < t \le t_{N_1} + \hat{\theta}_y$

$$\hat{Y} = \hat{Y}_{t_{P1}+\hat{\theta}_y} + \{\Delta Y^{\infty}(P_1,N_0,w_0,m_0;\hat{\beta}_y) - Y_{t_{P1}+\hat{\theta}_y} + Y_0\}g((t-\hat{\theta}_y-t_{P_1}),\hat{\tau}_y)$$

For $t_{N_1} + \hat{\theta}_y < t \le t_{P_2} + \hat{\theta}_y$

$$\hat{Y} = \hat{Y}_{t_{N1}+\hat{\theta}_y} + \{\Delta Y^{\infty}(P_1,N_1,w_0,m_0;\hat{\beta}_y) - Y_{t_{N1}+\hat{\theta}_y} + Y_0\}g((t-\hat{\theta}_y-t_{N_1}),\hat{\tau}_y)$$

For $t_{P_2} + \hat{\theta}_y < t \le t_{N_2} + \hat{\theta}_y$

$$\hat{Y} = \hat{Y}_{t_{P2}+\hat{\theta}_y} + \{\Delta Y^{\infty}(P_2,N_1,w_0,m_0;\hat{\beta}_y) - Y_{t_{P2}+\hat{\theta}_y} + Y_0\}g((t-\hat{\theta}_y-t_{P_2}),\hat{\tau}_y)$$

For $t > t_{N_2} + \hat{\theta}_y$

$$\hat{Y} = \hat{Y}_{t_{N2}+\hat{\theta}_y} + \{\Delta Y^{\infty}(P_2,N_2,w_0,m_0;\hat{\beta}_y) - Y_{t_{N2}+\hat{\theta}_y} + Y_0\}g((t-\hat{\theta}_y-t_{N_2}),\hat{\tau}_y) \quad (26)$$

As stated in section 2, H-BEST predictions require only the current change in the input values. Apart from minimal memory requirements, this property makes it attractive for computer coding for a real process.

8. The Study

In this section the predictive performance of the H-BEST algorithm is presented for the five outputs of the dryer process. The power and the fan speed are changed arbitrarily (i.e., randomly) as a series of step changes shown in Figure 12. The initial weight of the clothes and the moisture content for this study are 2.85 kg and 59.6%, respectively. H-BEST predictions using the input sequences in Figure 12 are shown in Figures 13−17, for the coil temperature, air temperature, surface temperature, wet bulb temperature, and dry bulb temperature, respectively.

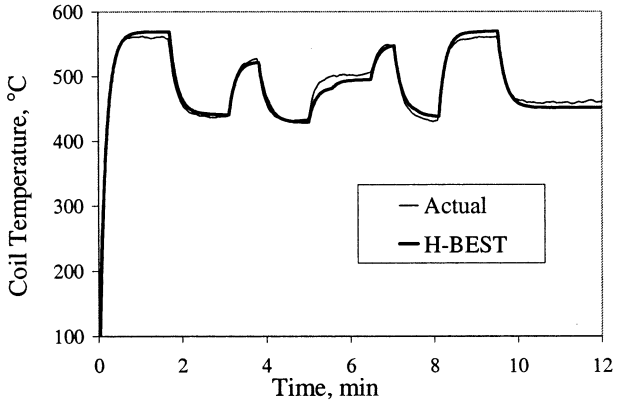

Figure 13. Coil temperature response to the input sequences shown in Figure 12.

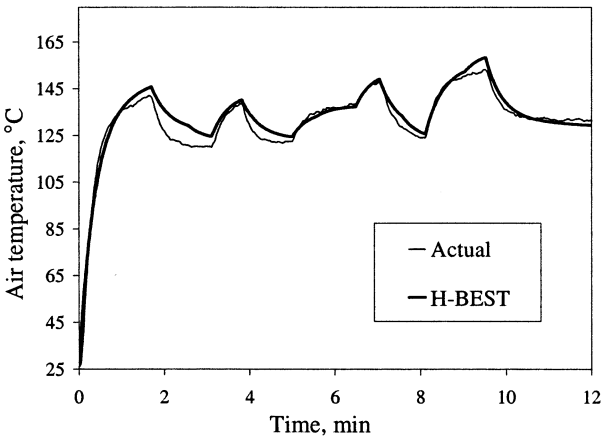

Figure 14. Heater exit air temperature response to the input sequences shown in Figure 12.

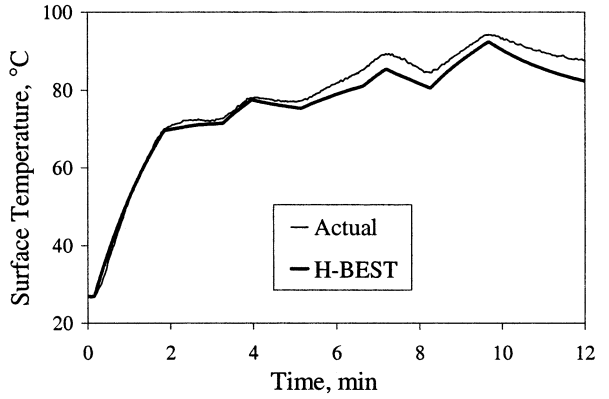

Figure 15. Heater surface temperature response to the input sequences shown in Figure 12.

The predictions from H-BEST closely follow the process at all times. The results clearly show an excellent performance. Thus, H-BEST appears to hold much promise of the accurate prediction of real dynamic MIMO processes.

9. Closing Remarks

This work presented a methodology to accurately model processes that behave as Hammerstein or approximate Hammerstein systems. We presented an exact closed-form solution to a Hammerstein system

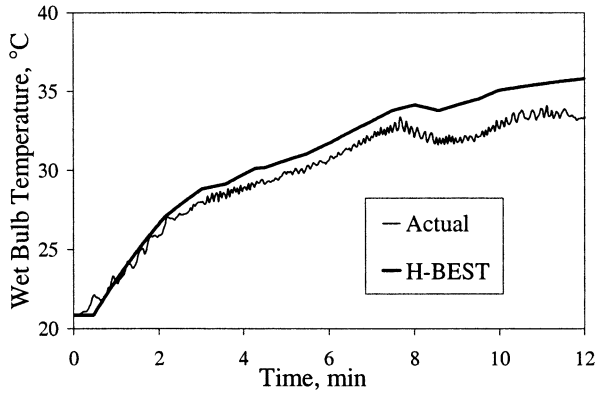

Figure 16. Dryer outlet wet bulb temperature response to the input sequences shown in Figure 12.

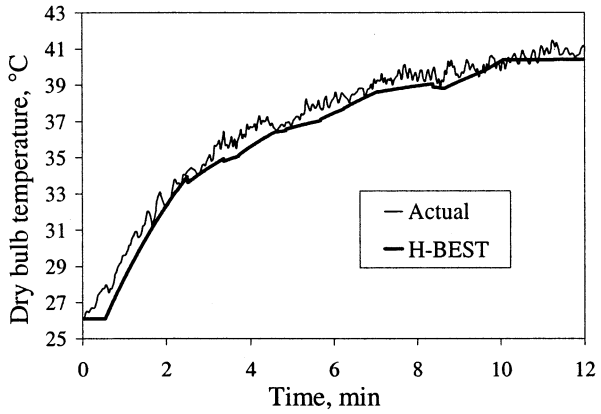

Figure 17. Dryer outlet dry bulb temperature response to the input sequences shown in Figure 12.

that was also useful in inspiring the model building methodology proposed. The effectiveness of this methodology was demonstrated on a mathematical model and a real process. It appears that Hammerstein modeling has seen much activity in discrete-time situations but limited application in continuous-time modeling. A critical reason that the proposed approach is successful is its ability to formulate output prediction in explicit form with separate terms for the steady and dynamic portions. Another key to its success is the ability of its prediction algorithm to achieve high accuracy with a series of input changes over time. This work extends the SISO method of Rollins et al.[1] to MIMO processes, and it is able to take full advantage of SDOE.

The accuracy of the proposed approach is dependent on the degree to which the process under consideration behaves as a Hammerstein process in the defined input space. It is also dependent on the degree to which the assumptions of the approach are satisfied as described in detail by the proof given in the appendix. The most critical of these assumptions is zero derivatives at input change points when the dynamics are not overdamped. To address this limitation, we are currently developing a modified algorithm of this method to account for nontrivial derivatives at change points. Another limitation of our proposed approach is the requirement for the input changes to be step changes. However, this limitation is less critical because, for high accuracy, the only necessary input change requirement is for the inputs to be approximated accurately by piecewise step functions. In research we have found this methodology to do quite well for highly complex continuous-input signals with sufficiently fast sampling times. In addition, we are also successfully extending this methodology to the exact treatment of common input types.

Our main motivation for selecting the dryer process for this study was to demonstrate the ability of the proposed approach to model a real system. It also shows the ability of the proposed methodology to address nonlinear and interactive behavior as demonstrated by the outputs in the dryer process. In addition, it demonstrates nicely the utilization of SDOE and the application of H-BEST to a real MIMO problem.

The proposed method has the potential to bring SDOE into the realm of dynamic processes. Current SDOE is taught and applied in the steady-state context. When processes are dynamic, the common practice is to allow the process to reach steady state and then collect the data. The proposed method gives a framework to teach and apply SDOE in a dynamic context.

Currently, we are investigating the evaluation of experimental designs using the D-optimality criterion. This has been made possible by our ability to write a compact closed-form solution for Hammerstein processes. Using the exact solution, we can generate the output response for processes with known (a priori) structure and evaluate the determinant of the derivative matrix for competing designs. Preliminary results from this work have clearly shown the superiority of step tests based on SDOE over the very popular method of pseudo random sequences.

Future work will also involve the development of continuous-time, predictive modeling methodologies based on exact solutions to other block-oriented structures such as the Wiener structure, the sandwich structure (a combination of Hammerstein and Wiener), and so on.

Acknowledgment

The authors acknowledge the partial support for the research by the National Science Foundation under Grant CTS-9453534 and by Frigidaire Corp., IEC (Iowa Energy Center), and CATD (Center for Advanced Technology Development). We are also grateful to the Program for Women in Science and Engineering at Iowa State University and Trisha Greiner for her assistance.

Appendix: Mathematical Proof of Equation 8

This appendix gives a mathematical proof of the H-BEST solution to the Hammerstein system under certain conditions. This proof is given by defining a rather general Hammerstein process and working forward to derive the H-BEST form (i.e., eq 8). One could also start from the H-BEST form and, using differential calculus, determine the process as originally given in differential form. In addition, other methods that one could use for this proof include the convolution method and the impulse response method. The proof is given here for step input changes for *n*th-order Hammerstein processes with only real poles and no restrictions and for other processes with restrictions (i.e., those with zeroes and complex poles). To begin this proof, we state the following assumptions:

1. The input changes are step changes, i.e., piecewise constant input changes.

2. The process has linear dynamics; i.e., the relationship between the inputs and the outputs can be described by a linear *n*th-order differential equation.

3. The $n-1$ derivatives of the output, dy/dt, d^2y/dt^2, ..., $d^{n-1}y/dt^{n-1}$ are zero at the time of the input change, i.e.,

$$\left.\frac{dy}{dt}\right|_{t_i} = \left.\frac{d^2y}{dt^2}\right|_{t_i} = \ldots = \left.\frac{d^{n-1}y}{dt^{n-1}}\right|_{t_i} = 0$$

Note that there is no restriction on the ultimate change function, i.e., $f(\mathbf{u}(t))$. The class of processes covered by the scope of this proof are as follows:

Class 1: nth-order stable processes with real poles.

Class 2: Stable processes with a transfer function consisting of p poles and q zeroes with $q < p$ and the condition that processes reach steady state after each input change.

The proof is shown here for an nth-order system with real and distinct poles (i.e., a subset of class 1). The inputs in any given interval $t_i \le t < t_{i+1}$, with $t_{i+1} > t_i$, are given by $\mathbf{u}(t) = \mathbf{u}(t_i)$. Mathematically this process can be written as

$$a_n\frac{d^n y(t)}{dt^n} + a_{n-1}\frac{d^{n-1}y(t)}{dt^{n-1}} + \ldots + a_1\frac{dy(t)}{dt} + y(t) = v(t)|_{t_i} \quad \text{(A1)}$$

where

$$v(t)|_{t_i} = v(t_i)\,\mathbf{S}(t-t_i) = f(\mathbf{u}(t_i))\,\mathbf{S}(t-t_i) \qquad \forall\, i \quad \text{(A2)}$$

and $\mathbf{S}(t-t_i)$ is the shifted unit step function. Let us define

$$y(t)|_{t_i} = y(t_i)\,\mathbf{S}(t-t_i) \quad \text{(A3)}$$

For the conditions of this proof, it can be shown that (proof omitted for space considerations but see Ogunnaike and Ray[23] for support)

$$\left.\frac{dy}{dt}\right|_{t_i} = \left.\frac{d^2y}{dt^2}\right|_{t_i} = \ldots = \left.\frac{d^{n-1}y}{dt^{n-1}}\right|_{t_i} = 0 \quad \text{(A4)}$$

Taking the Laplace transform of eq A1 gives

$$a_n[s^nY(s) - s^{n-1}y(t_i)\,e^{-t_is}] + a_{n-1}[s^{n-1}Y(s) - s^{n-2}y(t_i)\,e^{-t_is}] + \ldots + a_1[sY(s) - y(t_i)\,e^{-t_is}] + Y(s) = V(s)\,e^{-t_is} = \frac{f(\mathbf{u}(t_i))\,e^{-t_is}}{s} \quad \text{(A5)}$$

Rearranging the terms in eq A5 gives

$$[a_ns^n + a_{n-1}s^{n-1} + \ldots + a_1s + 1]Y(s) - [a_ns^{n-1} + a_{n-1}s^{n-2} + \ldots + a_1]y(t_i)\,e^{-t_is} = \frac{f(\mathbf{u}(t_i))\,e^{-t_is}}{s} \quad \text{(A6)}$$

Moving terms associated with $y(t_i)$ to the right-hand side (RHS) of eq A6 and dividing both sides by the term in front of $Y(s)$ gives

$$Y(s) = \frac{f(\mathbf{u}(t_i))\,e^{-t_is}}{s[a_ns^n + a_{n-1}s^{n-1} + \ldots + a_1s + 1]} + \frac{[a_ns^{n-1} + a_{n-1}s^{n-2} + \ldots + a_1]y(t_i)\,e^{-t_is}}{a_ns^n + a_{n-1}s^{n-1} + \ldots + a_1s + 1} \quad \text{(A7)}$$

Because the system consisted of n real and distinct poles, the polynomial in the denominator of the RHS of eq A7 can be rewritten as

$$a_ns^n + a_{n-1}s^{n-1} + \ldots + a_1s + 1 = (\tau_1s+1)(\tau_2s+1)\ldots(\tau_ns+1) = \prod_{i=1}^{n}(\tau_is+1) \quad \text{(A8)}$$

where $\tau_1, \tau_2, \ldots, \tau_n$ are the time constants of the system. Substituting eq A8 into eq A7 gives

$$Y(s) = \frac{f(\mathbf{u}(t_i))\,e^{-t_is}}{s\prod_{i=1}^{n}(\tau_is+1)} + \frac{[a_ns^{n-1} + a_{n-1}s^{n-2} + \ldots + a_1]y(t_i)\,e^{-t_is}}{\prod_{i=1}^{n}(\tau_is+1)} \quad \text{(A9)}$$

Applying partial fraction expansion to the terms on the RHS of eq A9 allows it to be rewritten as

$$Y(s) = f(\mathbf{u}(t_i))\,e^{-t_is}\left[\frac{A_0}{s} + \sum_{i=1}^{n}\frac{A_i}{(\tau_is+1)}\right] + y(t_i)\,e^{-t_is}\left[\sum_{i=1}^{n}\frac{B_i}{(\tau_is+1)}\right] \quad \text{(A10)}$$

where $A_0 = 1$.

$$A_i = \frac{-\tau_i^{\,n}}{\prod_{j=1,j\neq i}^{n}(\tau_i - \tau_j)} \quad \text{and} \quad B_i = \frac{\tau_i^{\,n}}{\prod_{j=1,j\neq i}^{n}(\tau_i - \tau_j)} \quad \text{(A11)}$$

We can see from eq A11 that $B_i = -A_i$. Taking the inverse Laplace transform of eq A10 and using $B_i = -A_i$ gives

$$y(t) = f(\mathbf{u}(t_i))\left[1 + \sum_{i=1}^{n}\frac{A_i}{\tau_i}\,e^{-(t-t_i)/\tau_i}\right]\mathbf{S}(t-t_i) - y(t_i)\left[\sum_{i=1}^{n}\frac{A_i}{\tau_i}\,e^{-(t-t_i)/\tau_i}\right]\mathbf{S}(t-t_i) \quad \text{(A12)}$$

Adding and subtracting 1 from the term after the $y(t_i)$ term in eq A12 gives

$$y(t) = \left\{f(\mathbf{u}(t_i))\left[1 + \sum_{i=1}^{n}\frac{A_i}{\tau_i}\,e^{-(t-t_i)/\tau_i}\right] - y(t_i)\left[1 + \sum_{i=1}^{n}\frac{A_i}{\tau_i}\,e^{-(t-t_i)/\tau_i} - 1\right]\right\}\mathbf{S}(t-t_i) \quad \text{(A13)}$$

Combining terms that contain A_i in eq A13 gives

$$y(t) = \left\{(f(\mathbf{u}(t_i)) - y(t_i))\left[1 + \sum_{i=1}^{n}\frac{A_i}{\tau_i}\,e^{-(t-t_i)/\tau_i}\right] + y(t_i)\right\}\mathbf{S}(t-t_i) \quad \text{(A14)}$$

Also, recognizing that

$$1 + \sum_{i=1}^{n}\frac{A_i}{\tau_i}\,e^{-(t-t_i)/\tau_i} = \mathcal{L}^{-1}\left(\frac{1}{s}G(s)\,e^{-t_i s}\right) = g(t-t_i) \quad \text{(A15)}$$

where

$$G(s) = \frac{Y(s)}{V(s)} = \frac{1}{(\tau_1 s + 1)(\tau_2 s + 1)...(\tau_n s + 1)} \quad \text{(A16)}$$

Substituting eq A15 into eq A14 and realizing that $\mathbf{S}(t-t_i) = 1$ (for $t > t_i$) gives

For $t > t_i$,

$$y(t) = y(t_i) + (f(\mathbf{u}(t_i)) - y(t_i))\,g(t-t_i) \quad \text{(A17)}$$

Because eq A17 is the same as eq 8, the proof follows. This proof was shown for an nth-order process with real and distinct poles. Without loss of generality, this proof can be extended to an nth-order process with real and identical poles. For processes with a dead time of θ, the H-BEST solution, i.e., eq 8 or eq A17, is modified by substituting $t_i + \theta$ for t_i in the arguments of $y(t_i)$ and $g(t-t_i)$. We are currently developing proofs for other cases (processes with poles and zeroes, with dead time, etc.) in research. In addition, for the class 2 cases (mentioned above), with significant derivatives at input change points, we are developing a modification to the method we have presented in this paper.

Nomenclature

f = ultimate change function
g = dynamic function
m = moisture content of the clothes
N = fan speed
P = power
t = time
T_a = air (exiting the heater) temperature
T_c = coil temperature
T_d = dry bulb temperature at the dryer outlet
T_s = surface temperature of the heater
T_w = wet bulb temperature at the dryer outlet
$\mathbf{u}$ = vector of input variables
$\Delta\mathbf{u}(t)$ = vector of input deviation variables from the nominal steady state
v = intermediate hidden variable in a Hammerstein model
w = dry weight of clothes in the dryer
y = output variable

Greek Letters

$\boldsymbol{\beta}$ = vector of parameter estimates for the ultimate change function for outputs
θ_i = dead time for the dynamic model, for output i
$\boldsymbol{\tau}$ = vector of dynamic parameters
τ_i = time constant for the dynamic model (first order) for output i
τ_{ik} = time constant for the dynamic model (second order) for output i where $k = a$, 1, or 2

Subscripts

a = air
c = coil
d = dry bulb
s = surface
w = wet bulb

Superscript

$\wedge$ = estimate

Abbreviations

FO = first order
FOPDT = first-order plus dead time
H-BEST = Hammerstein block-oriented exact solution technique
MIMO = multiple input, multiple output
SDOE = statistical design of experiments
SISO = single input, single output
SOPL = second-order plus lead
SOPLPDT = second-order plus lead plus dead time

Literature Cited

(1) Rollins, D. K.; Smith, P.; Liang, J. M. Accurate Simplistic Predictive Modeling of Nonlinear Dynamic Processes. *ISA Trans.* **1998**, *36*, 293.

(2) Ho, A. K.; Perera, J. M.; Dunstan, D. E. Measurement and Theoretical modeling of protein Mobility through Membranes. *AIChE J.* **1999**, *45* (7), 1434.

(3) Yang, C. J.; Jenekhe, S. A.; Meth, J. S. Probing structure-property relationships in third-order nonlinear optical polymers: third harmonic generation spectroscopy and theoretical modeling of systematically derivatized conjugated aromatic polyimines. *Ind. Eng. Chem. Res.* **1999**, *38* (5), 1759.

(4) He, X.; Liu, S.; Asada, H. A. Modeling of Vapor Compression Cycles for Multivariable Feedback Control of HVAC Systems. *J. Dyn. Syst., Meas., Control* **1997**, *119*, 183.

(5) Huang, B. J.; Ko, P. Y. A System Dynamics Model of Fire-Tube Shell Boiler. *J. Dyn. Syst., Meas., Control* **1994**, *116*, 745.

(6) Huang, B. J.; Wang, S. B. Identification of Solar Collector Dynamics Using Physical Model-Based Approach. *J. Dyn. Syst., Meas., Control* **1994**, *116*, 755.

(7) Holcomb, T. R.; Rhodes, C. A.; Morari, M. Input/Output Modeling for Process Control. In *Methods of Model Based Process Control*; Berber, R., Ed.; Kluwer Academic Publishers: Dordrecht, The Netherlands, 1995.

(8) Pottman, M.; Seborg, D. E. Identification of Nonlinear Processes using Reciprocal Multiquadratic Functions. *J. Process Control* **1992**, *2* (4), 189.

(9) Billings, S. A. Identification of Nonlinear Systems B: a Survey. *IEEE Proc.* **1980**, *127*, 272.

(10) Pearson, R. K.; Ogunnaike, B. A. Nonlinear Process Identification. In *Nonlinear Process Control*; Henson, M. A., Seborg, D. E., Eds.; Prentice Hall: Upper Saddle River, NJ, 1997.

(11) Chen, V. C. P.; Rollins, D. K. Issues Regarding Artificial Neural Network Modeling for Reactors and Fermenters. *J. Bioprocess Eng.* **2000**, *20*, 85.

(12) Eskinat, E.; Johnson, S. H.; Luyben, W. L. Use of Hammerstein Models in Identification of Nonlinear Systems. *AIChE J.* **1991**, *37* (2), 255.

(13) Rietz, C. A.; Rollins, D. K. Implementation of a Predictive Modeling Technique on a DCS. *Proceedings of the American Control Conference*, Philadelphia, PA, 1998; p 2951.

(14) Rollins, D. K.; McNaughton, M.; Schulze-Hewett, C. M. Accurate Semi-empirical Predictive Modeling of an Underdamped Process. *ISA Trans.* **1999**, *38*, 279.

(15) Walker, J. J. Development of an Empirical Model of Human Sweating and a Semi-empirical Model of Human Thermoregulation. Ph.D. Dissertation, Iowa State University, Ames, IA, 1999.

(16) Greblicki, W. Continuous-Time Hammerstein System Identification. *IEEE Trans. Autom. Control* **2000**, *45* (6), 1232.

(17) Montgomery, D. C. *Design and Analysis of Experiments*; John Wiley and Sons: New York, 1984.

(18) Bhandari, N.; Rollins, D. K. Superior Semi-empirical Dynamic Predictive Modeling that Addresses Interactions. Proceedings of the Intelligent Systems and Control Conference, Santa Barbara, CA, 1999.

(19) Rollins, D. K.; Bhandari, N. Accurate Predictive Modeling of Response Variables under Dynamic Condition without the Use of Past Response Data. *ISA Trans.* **2000**, *39*, 29.

(20) Haber, R.; Unbehauen, H. Structure Identification of Nonlinear Dynamic Systems B: A Survey on Input/Output Approaches. *Automatica* **1990**, *26* (4), 651.

(21) Wells, L. K.; Travis, J. *Lab View for Everyone*; Prentice Hall: Englewood Cliffs, NJ, 1997.

(22) Bhandari, N. Development of a new comprehensive predictive modeling and control framework for multiple-input, multiple-output processes. Ph.D. Dissertation, Iowa State University, Ames, IA, 2000.

(23) Ogunnaike, B. A.; Ray, W. H. *Process Dynamics, Modeling, and Control*; Oxford University Press: New York, 1994.

Received for review March 4, 2002
Revised manuscript received September 27, 2002
Accepted December 4, 2002

IE020169G